JOURNAL OF CATALYSIS 60, 156–166 (1979)

Controlled Pore Sizes and Active Site Spacings Determining Selectivity in Amorphous Silica–Alumina Catalysts

MARK R. S. MANTON[1] AND JOHN C. DAVIDTZ[2]

Chemical Engineering Research Group–CSIR, P.O. Box 395, Pretoria, South Africa

Received August 21, 1978; revised March 14, 1979

Controlled pore sizes in amorphous silica–alumina were achieved by employing tetraalkylammonium cations (TMA (methyl) to TBA (butyl)] as the *only* counterions to the fourfold coordinated aluminate ions in the gels. The width of the pore size distributions and the median size of the pores in the calcined silica–aluminas (now free of nitrogenous cations) decreased as the size of the cations used in the synthesis increased, except in the butyl case. The median values as determined by N_2 desorption were 15, 5, 4.5, 3.7, and 4.2 nm for the Na/NH_4–, TMA–, TEA–, TPA–, and TBA–silica–aluminas, respectively. The surface area per unit mass of catalyst increased with the size of the cations. The average interexchange site distance increased correspondingly, except in the butyl case. This exception is attributed to constraints set by the specific SiO_2/Al_2O_3 ratio used. In the catalytic cracking of heptane the TPA–silica–alumina produced substantially greater proportions of toluene and cyclic C_6 hydrocarbons than the other silica–aluminas. These materials have potential as sorbents, catalysts, and catalyst supports inter alia in the treatment of heavy residue and coal liquids where zeolites cannot be used because of their small pore sizes (<1 nm).

INTRODUCTION

The tendency toward heavier fossil fuel oils and higher oil prices has increased the interest in catalysts and catalyst supports which have pore sizes and catalytic properties optimized to cope with the large molecules (*1*).

Zeolites, for example, have proved to be efficient light oil cracking catalysts and have further potential as catalyst supports (*2*). However, access to active centers is limited to molecules whose size *and* shape permit their passage through the pore restrictions and openings (*3*, *4*). Reactant molecules larger than the critical dimensions (usually about 1 nm) (*5*) are excluded.

Recently amorphous silica–aluminas have been reported which have catalytic properties similar to those of zeolites but without the zeolite pore restrictions. These have been synthesized by:

- hydrolysis of bulky organosilanes in the presence of aluminum salts (*6*);
- the introduction of an aging step into the standard technique (*7*) of co-gela-aluminate (*8*) and;
- co-gelation of silica and alumina hydrosols in the presence of potassium ions (*9*).

Although tetraalkylammonium cations have been widely used in zeolite syntheses (*10*), they have not been reported as being

[1] Present address: Department of Chemical Engineering, M.I.T., Cambridge, Mass. 02139. To whom correspondence should be mailed.

[2] Present address: Department of Chemistry, University of Pretoria, Pretoria, South Africa.

0021-9517/79/130156-11$02.00/0

TABLE 1

Details of Reagents Used

Reagent	Source	Concentration or purity (as measured)
SiO_2	Degussa	99.88%
Al $(OH)_3$	Merck Suchart	98%
Tetraalkylammonium hydroxides		
Methyl (TMAOH)	Hopkins & Williams	26.6% by mass
Ethyl (TEAOH)	B.D.H.	26.9%
Propyl (TPAOH)	Fluka	18.9%
Butyl (TBAOH)	Fluka	36.7%
Hydrochloric acid	Merck (Titrisol)	1.0 *N*
NaOH	Merck (A. R. grade)	98%

used for the synthesis of amorphous silica–aluminas. When these cations were used the formulations also contained Na^+ or other cations. In the current work amorphous silica–aluminas were synthesized in the exclusive presence of a single species of tetraalkylammonium cation. This enabled the properties of the resultant silica–alumina to be related to the size of the cation used.

EXPERIMENTAL

The sources of reagents used and their concentrations are shown in Table 1.

SiO_2 (10 g) was dissolved in an equimolar amount of each tetraalkylammonium hydroxide (TAAOH), and in NaOH solution (to act as a control), by heating and stirring. The solution were diluted to give $[OH^-] = 0.93$ *M* (the concentration of hydroxide in the least concentrated tetrapropylammonium hydroxide solution). Half a gram of $Al(OH)_3$ was dissolved in a 10 *M* excess of each hydroxide solution by heating and stirring. All solutions were filtered, analyzed, and stored in polypropylene bottles.

The masses of alkali silicate and alkali aluminate required to give wet gels of similar composition were placed in a plastic beaker and stirred with a high-speed counter-rotating mixer. The predetermined amount of 1.0 *N* HCl was added using a tube pump, and the pH recorded until gelation occurred at pH 9. This occurred uniformly after all the acid had been added. The gels were aged at 25°C for 24 hr, filtered, and washed with deionized water until free of Cl^-, determined using $AgNO_3$ solution. The samples were dried at 60°C for 48 hr and then at 110°C for a further 48 hr at atmospheric pressure.

The silica–alumina synthesized in the presence of sodium cations was ion-exchanged three times under reflux with 3 *M* NH_4Cl and washed free of Cl^- ions prior to drying.

The mass loss on ignition to 1000°C and the SiO_2 content were determined gravimetrically. The Al_2O_3 content was determined by volumetric titration with ethylenediaminetetraacetic acid (EDTA) and zinc solution. After ion exchange with NH_4Cl the silica–alumina synthesized in the presence of Na cations was tested for residual Na content by atomic absorption.

The thermogravimetry of each sample was determined on a DuPont 990 thermal analyzer under a N_2 flow of about 150 cm^3 min^{-1}. The tetraalkylammonium cations decompose releasing alkaline material, probably in a manner analogous to that for

tetramethylammonium cations (*11*);

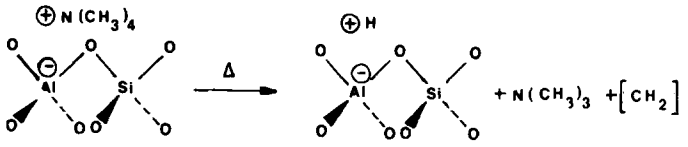

The release of alkaline decomposition products with temperature was recorded, using the method of Kerr and Chester (*12*) by absorption in a solution of 15 cm^3 NH_4Cl and 1 cm^3 saturated boric acid in the reaction vessel of a Radiometer titration assembly. The pH of the solution was kept constant at pH 5.0 by the incremental addition of 5.872 mmol $liter^{-1}$ sulfamic acid.

The cation-exchange capacities of the calcined gels were determined by NH_3 desorption after ion exchange with NH_4Cl (*12*).

The surface areas were determined by BET N_2 adsorption and the pore size distributions by N_2 desorption and by mercury porosimetry. Samples of the dry gels ground to <150 μm were calcined by heating at a controlled rate of just less than 1°C min^{-1} under an atmosphere of nitrogen (flow rate, ca. 20 cm^3 min^{-1}). Samples of 0.2 g were removed at 25°C intervals from 450°C and tested for dehydration activity (*13*, *14*) on refluxing tertiary butanol to evaluate the profile of pretreatment temperature versus activity.

The dried gels (ground to 500–700 μm) were calcined to 560°C, the experimentally found optimum pretreatment temperature for tertiary butanol dehydration. The changes in product selectivities during isothermal catalytic conversion (at 450°C) of *n*-heptane on calcined gels were recorded against time. Nitrogen carrier gas (6.0 cm^3 min^{-1}) was bubbled through *n*-heptane, then passed through a preheater coil in a fluidized sand bath before contacting 0.4 g of catalyst in a 50 × 4.3-mm-i.d. ($\frac{1}{4}$-in.-o.d.) stainless-steel microreactor. This resulted in a superficial contact time of about 10 s which represents a conventional magnitude for contact time in cracking tests (*15*).

The products from the reactor were sampled using the heated gas sampling valve (2.0 cm^3) of a Hewlett–Packard 5830A gas chromatograph. The products were separated over a 4-m × 2.1-mm-i.d. ($\frac{1}{8}$-in.-o.d.) stainless-steel chromatographic column packed with 10.6 mass% OV 101 on 100–120 mesh Chromosorb P-AW and analyzed using a flame ionization detector.

Since cracking of *n*-heptane over silica–alumina obeys pseudo-first-order kinetics (*15*), the rate constant κ for *n*-heptane conversion could be calculated using:

$$\kappa = \frac{1}{\tau} \ln \frac{1}{1 - \epsilon},$$

where τ is the contact time given by

$$\tau = \frac{\text{volume of catalyst}}{\text{gas flow rate}} \times \frac{\text{room temperature (K)}}{\text{reaction temperature (K)}},$$

and ϵ is the fractional conversion given by

$$\epsilon = \frac{[C_7]_i - [C_7]_f}{[C_7]_i},$$

where $[C_7]_i$ is the initial concentration of *n*-heptane and $[C_7]_f$ is the concentration of *n*-heptane after the reaction. The area percentage of each component in the product gas was automatically calculated by a microprocessor in the glc. The area percentage for heptane was used as an approximation for its concentration in calculating the rate constants.

TABLE 2

Molar Compositions of the Wet Gels Based on Masses Used in the Preparation and of the Dried Gels Based on Chemical Analysis

Cation used	Wet gel				Dry gel SiO_2/Al_2O_3
	SiO_2/Al_2O_3	OH^-/SiO_2	HCl/OH^-	H_2O/SiO_2	
Na/NH_4	80.6	1.25	0.852	117	66.9
TMA	80.7	1.32	0.824	123	98.6
TEA	79.2	1.27	0.845	119	90.2
TPA	80.6	1.33	0.881	130	95.5
TBA	80.3	1.28	0.968	130	92.5

RESULTS AND DISCUSSION

Based on the masses of each compound used in the preparation (Table 2) the composition of the wet gels was nearly identical. The SiO_2/Al_2O_3 ratios of the dried gels as determined by chemical analysis were more widely scattered than those of the wet gels. This was probably due to experimental difficulties in the analysis of small quantities of Al_2O_3 in the SiO_2 matrices.

With the exception of the silica–alumina synthesized in the presence of Na cations, the SiO_2/Al_2O_3 ratio was higher in the dry gels. This may be an experimental variable but more probably indicates that some Al was washed from the matrix during the filtration/washing stages. The reason for the decrease in the SiO_2/Al_2O_3 ratio in the Na/NH_4 sample is unknown.

The X-ray powder diffraction pattern of each silica–alumina (ground to $<150\ \mu m$) was recorded between 30° and 2° 2θ. The spectra showed the samples to be amorphous to X rays. There was therefore no

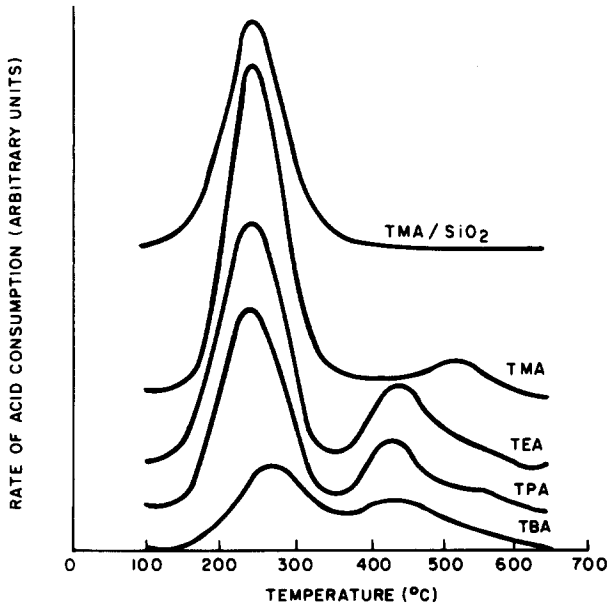

FIG. 1. Rate of acid consumption by tetraalkylammonium decomposition products with temperature.

TABLE 3

Concentration of Aluminum in the Catalysts after Calcination to Remove the Organic Cations, as Determined by Cation-Exchange Capacity (C.E.C.) and Chemical Analysis (C.A.)

Cation used	[Al] by C.E.C. (mmol g^{-1})	[Al] by C.A. (mmol g^{-1})	[Al] by C.E.C./ [Al] by C.A. (%)
Na/NH_4	0.14	0.49	30
TMA	0.20	0.33	60
TEA	0.25	0.36	69
TPA	0.23	0.34	67
TBA	0.25	0.35	70

indication of crystalline zeolite material being present.

Thermogravimetry

On heating silica–alumina synthesized in the presence of tetraalkylammonium hydroxide (TAA), alkaline decomposition products were released over two temperature ranges: 150 to ca. 350°C (median, 240°C) and ca. 350 to 650°C (Fig. 1). Pure silica gel synthesized under identical conditions, using tetramethylammonium hydroxide (TMA/SiO_2), only released decomposition products between 100 and 350°C. The TMA/SiO_2 contained no aluminum, therefore these products must have arisen from TMA cations occluded in the SiO_2 gel, and stabilized by it (solid TMAOH decomposes between 135 and 140°C (*16*)).

The presence of aluminum in the silica–aluminas stabilized some tetraalkylammonium cations to the extent that they only decomposed between 350 and 650°C. These cations were probably ionically bonded to the alumina anions in the silica framework.

The temperature ranges for the tetramethylammonium cation decompositions (350–650°C) agreed with literature values for TMA zeolites (*11*, *17*): 450 to 650 and 375 to 550°C, respectively.

Cation-Exchange Capacity and Surface Concentration of Al^{IV}

Only tetrahedrally coordinate aluminum (Al^{IV}) has cation exchange capacity (and strong-acid catalytic activity) (*18*) and so is able to ionically bind NH_4^+ cations.

TABLE 4

Surface Areas (S.A.) of the Silica–Aluminas and the Square Root of the Areas per Al Atom

Cation used	S.A. before calcination	S.A. after calcination	$(S.A.)^{\frac{1}{2}}$/C.E.C. Al[a] (nm Al^{-1})	$(S.A.)^{\frac{1}{2}}$/C.A. Al[b] (nm Al^{-1})
Na/NH_4	113	120	1.19	0.64
TMA	302	460	1.95	1.52
TEA	376	597	1.99	1.65
TPA	395	691	2.24	1.83
TBA	445	650	2.09	1.75

[a] Square root of the surface area after calcination, per Al atom; based on the cation exchange capacity value for [Al].

[b] Square root of the surface area after calcination, per Al atom; based on the chemical analysis (C.A.) value for [Al].

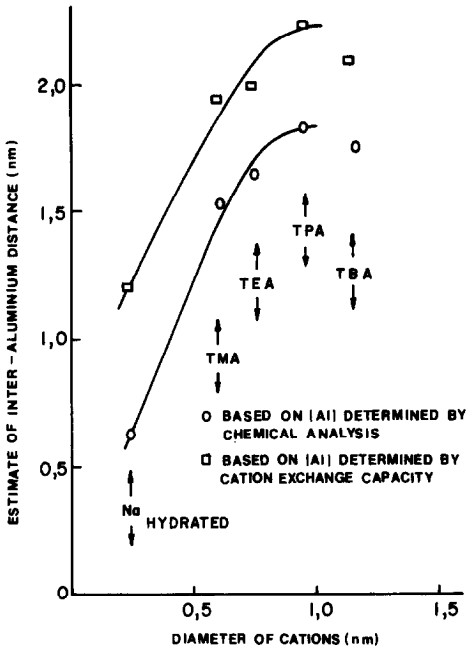

FIG. 2. The increase in interaluminum distance does not progress beyond that in the TPA–alumina–silica.

There is therefore a one-to-one correlation between the NH_3 released on heating an NH_4Cl-exchanged silica–alumina, and the concentration of Al^{IV} atoms on the surface accessible to NH_4^+ cations during the exchange, i.e., the cation-exchange capacity (C.E.C.) gives a measure of the Al^{IV} surface concentration (Table 3).

The concentrations of aluminum as determined by C.E.C. were all lower than the chemical analysis results. This may be ascribed to: (a) aluminum ions being washed from the SiO_2 framework during ion-exchange with NH_4Cl prior to the C.E.C. measurement, or (b) some of the aluminum being present in octahedral coordination. The Na/NH_4 was not as thermally stable as the tetraalkylammonium silica–aluminas and thus may have lost C.E.C. during calcination prior to C.E.C. determination.

Surface Properties

The bulky organic cations blocked pores and resulted in a lower surface area before calcination (Table 4).

The square root of the surface areas, after calcination, was divided by the concentration of aluminum in each sample as measured by chemical analysis or cation-exchange capacity (Table 4) to obtain an estimate of the *average* distance between Al atoms. The average distance increases with the size (from space filling models) of the cations used in the preparations (Fig. 2).

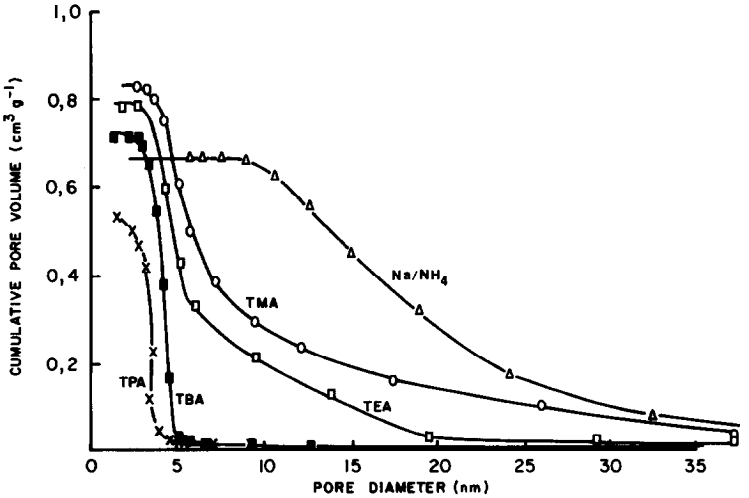

FIG. 3. Pore size distribution determined by N_2 desorption.

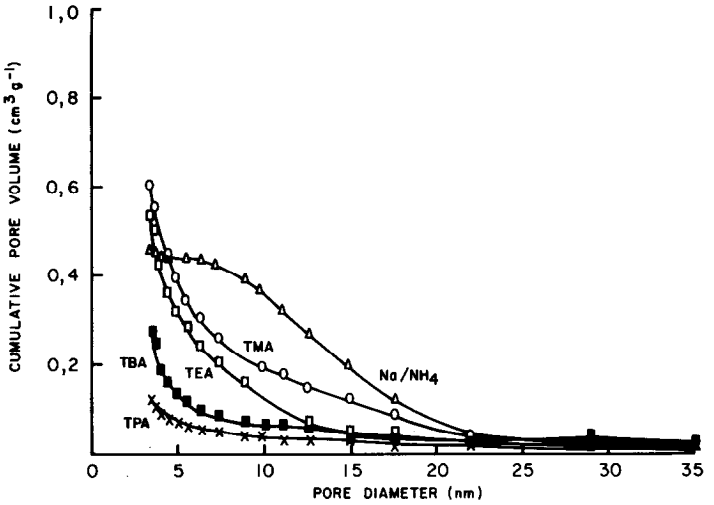

FIG. 4. Pore size distribution determined by mercury porosimetry.

The increase, with the exception of the TBA silica–alumina, probably arises from a combination of: (*a*) *coulombic repulsions*—the cations associated with the alumina anions during synthesis repel each other; and (*b*) *steric interferences*—the cations act as inert fillers decreasing the density and increasing the surface area per unit mass.

Since equimolar amounts of hydroxide were used in the synthesis rather than equal mass percentages, the larger the cation the greater the mass percentage of tetraalkyl cation, the lower the density and consequent higher surface area.

A tentative explanation for the TBA silica–alumina having a smaller surface area than the TPA silica–alumina is that in the latter all the silica molecules would fill the surface between the aluminas. When the slightly larger TBA cations are used the aluminums may not be able to be separated further because the maximum interaluminum distance for the particular SiO_2/Al_2O_3 ratio used (80/1) has been reached in the synthesis of the TPA silica–alumina.

Pore Size Distributions

The pore size distributions determined by N_2 desorption and mercury porosimetry agreed qualitatively with each other and with the surface area measurements: the higher the surface area the more small pores there are in the samples (Figs. 3 and 4). In the TPA silica–alumina the final cumulative pore area as determined by nitrogen desorption (652 m^2 g^{-1}) was less than the BET surface area (691 m^2 g^{-1}); the low pore size end of the curve in Fig. 3 does not reach a horizontal plateau, and it is likely that there are a few pores in the TPA silica–alumina smaller than indicated in Figs. 3 and 4.

The derivatives of the pore size distributions (Fig. 5) indicate that when tetraalkylammonium cations are used alone, the median size of the pores obtained is inversely related to the size of the cations used. These pores lie outside the zeolitic range (up to 1 nm) (*5*) and the silica–aluminas would therefore be more suitable as catalysts and catalyst supports where zeolites are unsuitable, e.g., in the treatment of coal liquids and where a narrow pore size distribution at about 3 nm is preferred.

The Activity versus Pretreatment Temperature Profile for t-Butanol Dehydration

In each catalyst the rate for t-butanol dehydration, often used for activity deter-

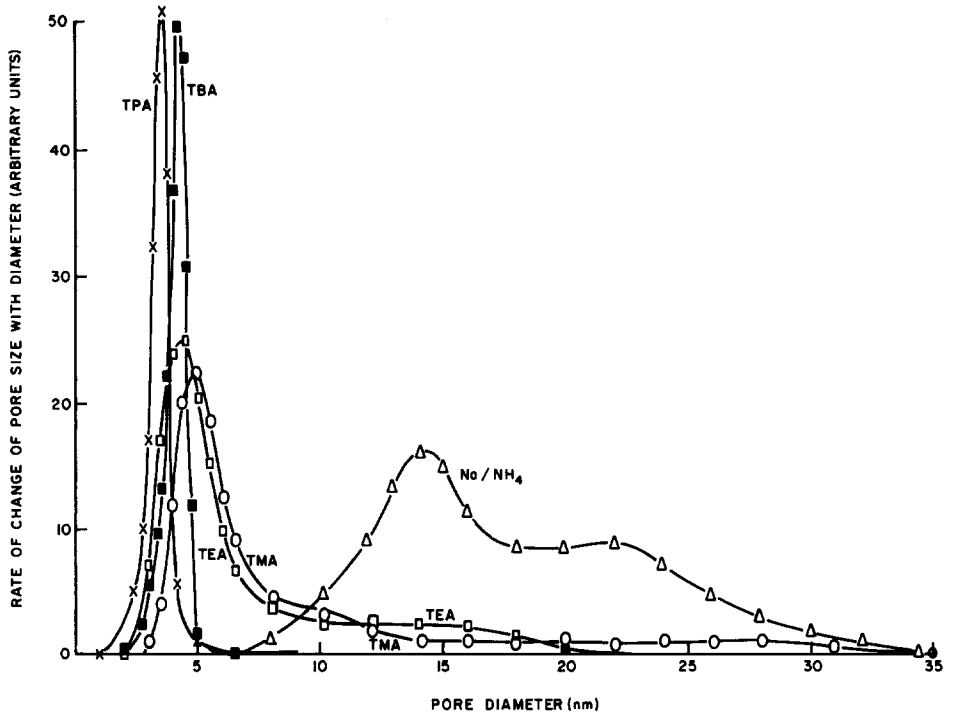

FIG. 5. Pore size distribution of catalysts, from N_2 desorption.

mination (*18*), increases from the value at the minimum pretreatment temperature, reaches a maximum activity at 500–580°C, and then decreases (Fig. 6).

Prior to calcination the catalysts contained the tetraalkylammonium cations which blocked the pores and screened the catalytic sites. When the catalysts were calcined to about 250°C the occluded cations were burned out but not those associated with the catalytic sites (Fig. 1). The gradual increase in the rate of t-butanol dehydration for the pretreatment temperature above 400°C arises from the removal of the cations bonded to the aluminum, resulting in the formation of Brønsted acid sites (*11*).

The dehydration of t-butanol requires catalysis by a proton (*13*). Therefore, dehydration of Brønsted acid sites into Lewis acid sites accounts for the decrease in the rate of reaction when the catalysts are preheated to >560°C. The sharpness of the peaks is caused by the catalysts beginning to dehydroxylate (which decreases the conversion rate) before all the cations have been removed (which would increase this rate).

Within the limits of experimental accuracy the pretreatment temperature that gives the maximum t-butanol dehydration rate increases with the size of the cation used (Fig. 6).

The dehydroxylation of silica–alumina involves either an OH group and an H atom from the *same* aluminum atom bound to the silica network through two oxygen bridges (*19*), or an OH group and an H atom from *adjacent* aluminum atoms bound to the silica network by three oxygen bridges (*20*).

If the former is the case no increase in the dehydroxylation temperature would be expected. If the latter applies, the increase indicates that the interexchange site distance increases with the size of the cations

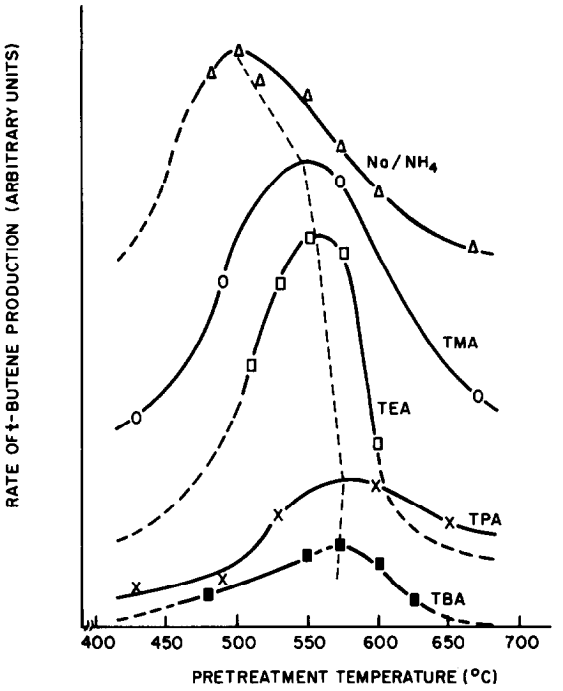

FIG. 6. The pretreatment temperature corresponding to maximum rate of t-butanol dehydration depends on the size of the cation used.

used, confirming the conclusion drawn from the surface area per site results.

Heptane Cracking and Product Selectivity

Rate constants for the TMA and Na/NH_4 catalysts were determined between 440 and 480°C. Activation energies of 28.1 and 30.5 kcal mol^{-1} were obtained, respectively. These agreed with the activation energy of 30 kcal mol^{-1} obtained by Miale *et al.* (*15*) for the catalytic cracking of hexane and octane over various amorphous silica–alumina and zeolite catalysts.

All catalysts had comparable concentrations of aluminum ions (Table 2), yet had different initial and final rate constants for the catalytic cracking of heptane at 450°C (Table 5). On the basis of the t-BuOH dehydration activities, each catalyst was pretreated to 560°C (except Na/NH_4 which was pretreated to 525°C). At this temperature there will still be cations blocking some of the catalytic sites (Fig. 1) causing the activity differences.

The individual peaks in the gas chromatograph were identified by their retention times and by spiking, and their area percentages calculated automatically by the instrument. Although area percentage values can differ by up to 20% from the molar percentage values, this can be ignored when the conversions to identical products by the different catalysts are being compared.

The Na/NH_4 catalyst was a better methanation—but worse cyclization—catalyst than the others, producing more straight chain C_6 and less cyclic C_6 molecules (Table 5). The TPA catalyst was extraordinarily active for toluene and cyclic C_6 production (Table 5). For comparison, results obtained with a 10% Al_2O_3 commercial silica–alumina catalyst [Kali Chemie, KC perlkator] are given.

CONCLUSIONS

In a novel synthesis technique for silica–aluminas using tetraalkylammonium

TABLE 5

Rate Constants and Product Selectivity Data for the Cracking of Heptane over the Catalysts[a]

Cation used	Rate constant (s^{-1})	Heptane unconverted (%)	Relative area% of converted products					
			C_1–C_3	C_4	C_5	Acyclic C_6	Cyclic C_6	Toluene (C_7)
		Time on stream = 7 min						
TMA	5.2	95.4	34	33	8	<1	4	20
TEA	6.6	93.8	40	33	7	<1	4	16
TPA	5.4	87.9	33	29	6	<1	6	26
TBA	4.0	95.7	34	38	4	<1	3	20
Na/NH_4	2.8	96.5	29	36	4	5	2	24
SiO_2/ 10% Al_2O_3	4.9	95.0	33	37	33	2	3	21
		Time on stream = 140 min						
TMA	3.3	97.0	39	43	4	2	—[b]	12
TEA	4.2	96.0	42	44	4	<1	—[b]	9
TPA	3.1	95.6	37	42	4	1	<1	17
TBA	2.5	97.3	38	44	4	1	—[b]	13
Na/NH_4	1.9	97.6	37	40	4	7	—[b]	13
SiO_2/ 10% Al_2O_3	2.8	97.2	34	43	6	3	—[b]	12

[a] For time on stream = 7 and 140 min, temperature = 450°C, contact time = approx. 10 s.
[b] Sample too small to be resolved.

cations as the only cations present, the median pore size and the broadness of the pore size distribution decreased with an increase in the size of the cations used.

This technique makes it possible to tailor-design the pore size distribution of silica–alumina catalysts and supports in certain size ranges. For Na/NH_4–, TMA–, TEA–, and TPA–silica–alumina the surface area per aluminum atom and consequently the average spacing of the active sites increased approximately linearly with the size of the cation used. The increase does not extend to the TBA case; this is attributed to the inability to obtain further spacing of the Al atoms with the specific SiO_2/Al_2O_3 ratio used.

Cracking *n*-heptane the TPA silica–alumina produced a higher proportion of toluene and other cyclic C_6's than the other catalysts.

ACKNOWLEDGMENTS

Thanks are due to Mr. J. Stander for the surface areas and N_2 desorption pore size distributions and to Dr. R. de Haan for the mercury porosimetry work. The M.Sc. thesis work on which the paper is based was carried out under the supervision of Professor C. J. H. Schutte, University of South Africa, and of Dr. J. C. Davidtz.

REFERENCES

1. Oblad, A. G., *Catal. Rev. Sci. Eng.* **14**, 83 (1976).
2. Leith, I. R., *Chemsa* **4**, 72 (1978).
3. Davidtz, J. C., "Proc. 2nd Nat. Meet. S.A. Inst. Chem. Eng., Johannesburg, South Africa, August 1976."
4. Becker, K. A., Karge, H. G., and Streubel, W. D., *J. Catal.* **28**, 403 (1973).
5. Venuto, P. B., and Hamilton, L. A., *Ind. Eng. Chem. Prod. Res. Develop.* **6**, 190 (1967).
6. Mitchell, T. O., and Whitehurst, D. D., U.S. Patent 4,003,825, January 18, 1977.
7. Plank, C. J., and Drake, L. C., *J. Coll. Sci.* **2**, 399 (1947).

8. Magee, J. S., and Daugherty, R. P., U.S. Patent 3,912,619, October 14, 1975.
9. Vaughan, D. E. W., Maher, P. K., and Albers, E. W., U. S. Patent 3,838,037, September 24, 1974.
10. Breck, D. W., "Zeolite Molecular Sieves." Wiley, New York, 1974.
11. Whyte, T. E., Wu, E. L., Kerr, G. T., and Venuto, P. B., *J. Catal.* **20**, 88 (1971).
12. Kerr, G. T., and Chester, A. W., *Thermochim. Acta* **3**, 113 (1971).
13. Frillette, V. J., Mower, E. B., and Rubin, M. K., *J. Catal.* **3**, 25 (1964).
14. Ignace, J. W., and Gates, B. C., *J. Catal.* **29**, 292 (1973).
15. Miale, J. N., Chen, N. Y., and Weisz, P. B., *J. Catal.* **6**, 278 (1966).
16. Musker, W. K., *J. Amer. Chem. Soc.* **86**, 960 (1964).
17. Aiello, R., and Barrer, R. M., *J. Chem. Soc. A*, 1470, 1970.
18. Davidtz, J. C., *J. Catal.* **43**, 260 (1976).
19. Bourne, K. H., Cannings, F. R., and Pitkethly, R. C., *J. Phys. Chem.* **74**, 2197 (1970).
20. Uytterhoeven, J. B., Christner, L. G., and Hall, W. K., *J. Phys. Chem.* **69**, 2117 (1966).